**Rare Metal Materials and Engineering**
Volume 49, Issue 8, August 2020
Available online at www.rmme.ac.cn

Science Press

**Cite this article as:** Rare Metal Materials and Engineering, 2020, 49(8): 2583-2590.

ARTICLE

# Effect of Bias Voltage on Microstructure and Erosion Resistance of CrAlN Coatings Deposited by Arc Ion Plating

**Wang Di[1,2], Lin Songsheng[2], Liu Lingyun[2], Xue Yuna[1], Yang Hongzhi[2], Jiang Bai-ling[1], Zhou Kesong[1,2]**

*[1] Xi'an University of Technology, Xi'an 710048, China; [2] The Key Lab of Guangdong for Modern Surface Engineering Technology, National Engineering Laboratory For Modern Materials Surface Engineering Technology, Guangdong Institute of New Materials, Guangzhou 510651, China*

**Abstract:** CrAlN coatings were prepared on TC11 titanium alloy by arc ion plating. The effects of negative bias voltage on the microstructure and mechanical properties, such as hardness and elastic modulus, of the coatings were investigated by X-ray diffraction (XRD), scanning electron microscope (SEM), energy dispersive X-ray spectroscopy (EDS) and nano-indentation. A series of solid particle erosion experiments were also conducted to study the influence of bias voltages on the solid particle erosion resistance of CrAlN coatings. Results show that the preferred growth orientation of CrA1N coatings gradually varies from (200) to (111) crystal plane with changing the bias voltage from 0 V to 200 V. The hardness increases from 15.1 GPa to nearly 20 GPa. At the same time, the number of macro-particles and pinholes decreases as the surface gradually flattens, which improves the erosion resistance of the CrAlN coating. The CrAlN coating deposited at the bias voltage of 150 V obtains the minimum erosion rates, which are 0.032 μm/g at 30° and 1.869 μm/g at 90°. These results indicate that the CrAlN coating formed at an appropriate bias voltage can achieve excellent solid particle erosion resistance.

**Key words:** CrAlN coating; negative bias voltage; microstructure; solid particle erosion

For the duration of an aircraft taking off, landing or flying at a low altitude, many irregular fine sands and dust inevitably enter the engine along with air flow. These high speed sand and dust will rub against the compressor blades, resulting in severe erosion damage of the blades. The design service life of the impeller is about 2200 h, but in this case it can only last about 300 h [1]. Up to now, there have been several approaches to reduce the erosion loss resulted from solid particle erosion (SPE) and to improve the service life of the components. Among them, the erosion resistant coatings are considered as potential way to solve such problem[2,3]. In different coating systems, some hard coatings have been found to be extremely resistant to SPE impact damage[4,5]. They are mainly divided into two coating series: (1) TiN-based systems including TiN, TiAlN, TiCN, TiSiN, TiSiCN, and many multilayer variations[6], and (2) carbon-based systems including diamond, diamond-like carbon (DLC) and tetrahedral amorphous carbon (ta-C)[7,8].

The hard coating has a certain protective effect. However, the toughness and high temperature oxidation of the hard coating are poor. Many researchers have conducted relevant research so as to improve the erosion resistance of coatings. Reedy[6] et al proved that the erosion resistance of (Ti,Cr)N nano-coating is highly dependent on the thickness and chromium contents in the coating. As the volume of CrN phase increases, the coating hardness decreases. At 30° erodent impingement, all the coated samples are superior to the bare substrate, whereas at 90° impingement, only the coatings deposited at low bias values (25, 50, and 100 V) with lower hardness are outstanding compared to the bare substrate.

Received date: August 21, 2019
Foundation item: Guangdong Science and Technology Program (2017A070701027, 2014B070705007); GDAS' Project of Science Technology Development (2019GDASYL-0302012, 2017GDASCX-0111)
Corresponding author: Zhou Kesong, Ph. D., Professor, School of Materials Science and Engineering, Xi'an University of Technology, Xi'an 710048, P. R. China, Tel: 0086-29-61086553, E-mail: kszhou2004@163.com

In addition, it has been generally acknowledged that the difference in hardness between hard coatings and titanium alloy substrate is harmful for their adhesion strength, which even reduces the fatigue lifetime of substrate. Meantime, the fracture rate is promoted under high stress conditions[9]. Therefore, the hardness does not play a major role in the erosion resistance of the coating. However, it has been inferred from the contact dynamics that the surface of the coating should have a small tensile contact stress by reducing the surface stiffness, unless the material has sufficient toughness to overcome the increase in stress[10]. So the erosion resistant material which possesses the high fracture toughness, moderate hardness and elastic modulus should be selected.

The toughness of the coating comes to be the key factor for further erosion application. The single-layer of CrN coating with a thickness up to 20 μm can be obtained, indicating that the toughness is much higher than that of the TiN coating with a maximum thickness of 5 μm. Meanwhile, some researchers[11] pointed out that Cr under-layer is certified to refine the upper-layer microstructure and enhance the bonding energy between the substrate and the buffer-layer. The CrN coating cannot meet the requirements of high temperature environment while the temperature requirement at the outlet of the engine compressor is getting increasingly higher. Therefore, the ternary compounds can be obtained by adding Al element so as to further improve the anti-oxidation of TiN and CrN coating[12].

In this work, the deposition, microstructure, mechanical properties and erosion resistance of CrAlN coatings on titanium alloy were systematically investigated. Furthermore, the hardness and toughness of the SPE coating were adjusted by Cr-based toughening and Al-doping hardening, and the influence of bias voltage on the erosion resistance of coatings was discussed in detail.

## 1 Experiment

### 1.1 CrAlN coatings preparation

The CrAlN coatings were deposited by the AS700DTX automatic control vacuum cathode arc deposition equipment. There are totally 8 circular targets in the chamber, 4 of which are chromium (99.9 wt%) and the other 4 composite ones are Cr0.5Al0.5 alloy (99.9 wt%, Cr and Al content are 50%). The substrate materials were silicon, YG6 tungsten steel (WC: 94%, Co: 6%) and TC11 titanium alloy (5.8~7.0 Al, 2.8~3.8 Mo, 0.8~2.0 Zr, 0.2~0.35 Si, wt%). The coatings deposited onto silicon substrates were used to test the phase composition and observe the surface and cross-section morphology. The coatings deposited onto YG6 cemented carbide substrates were used to test the hardness and elastic modulus. The coatings deposited onto TC11 titanium alloy substrates were applied to study the erosion resistance and observe the erosion scars.

All the substrate specimens were ground and polished to an average surface roughness of $R_a$<0.4 μm, and then ultrasonically cleaned in 5 vol% metal cleaner for 15 min. Subsequently, they were rinsed in deionized water to remove residual organic contaminates and dried by dehydrogenation drying equipment.

Prior to deposition, the vacuum in the chamber was about $10^{-3}$ Pa. The substrates were plasma cleaned through high purity (99.999 vol%) Ar at a high bias voltage of −1000 V for 25 min. To improve the adhesion between the coating and the substrate, the Cr and CrN layers were deposited at 100 A for 20 min as a buffer of the following CrAlN coatings. As for CrAlN coatings, the CrAl cathode arc current was set as 90 A at 300 °C for 2 h. The flow rates of nitrogen and argon were 500 and 100 mL/min, respectively, to maintain the pressure in the vacuum chamber at 4 Pa. The variation range of bias voltage was 0, 50, 100, 150 and 200 V with a duty ratio of 90±0.5%. The parameters and mechanical properties of CrAlN coating are listed in Table 1.

### 1.2 Microstructure characterization

The surface, cross-section morphologies and chemical composition of CrAlN coatings were revealed by scanning electron microscope (Nova Nano SEM 430) equipped with an energy dispersive X-ray spectroscopy (EDS). The crystal structures of the coatings were characterized by X-ray diffraction (XRD, Philips X'Pert3 Powder) from 10° to 90° at an increment of 0.02°. The hardness ($H$) and elastic modulus ($E$) were determined by a Nano-Test 600 nano-mechanical system (Micro-Materials Ltd, UK). The indentation depth was 200 nm with a maximum load of 50 mN. An average of 25 repeated indentations was taken for each specimen.

### 1.3 Sand particle erosion experiment

The sand erosion experiments were conducted under a self-designed AS600 sandblasting test machine as per ASTM G76-13standard[13], and corresponding setup is schematically shown in Fig.1. Based on preliminary experiment, the particle velocity was controlled at (30±2) m/s, and the working distance between specimen and the outlet of nozzle was 10 mm. The impingement angle was set as 30° and 90°. The depth of erosion pits was measured by Bruker DEKTAX profile-meter. The solid abrasive particles of the erosion test

**Table 1 Parameters, composition and mechanical properties of CrAlN coatings**

| Sample | Bias voltage/V | Thickness/μm | Adhesion/N | $X_{Cr}$/at% | $X_{Al}$/at% | Ratio of Al:(Cr+Al) | Hardness/GPa | Elastic modulus/GPa |
|---|---|---|---|---|---|---|---|---|
| CrAlN-1 | 0 | 2.74 | 32.8 | 28.22 | 19.68 | 0.411 | 15.1 | 256.4 |
| CrAlN-2 | 50 | 2.57 | 35.4 | 30.20 | 19.38 | 0.391 | 16.1 | 266.8 |
| CrAlN-3 | 100 | 2.14 | 41.0 | 25.54 | 19.94 | 0.438 | 18.6 | 254.0 |
| CrAlN-4 | 150 | 2.28 | 42.6 | 25.31 | 20.43 | 0.447 | 20.0 | 259.3 |
| CrAlN-5 | 200 | 2.16 | 41.4 | 24.18 | 20.78 | 0.462 | 19.1 | 256.4 |

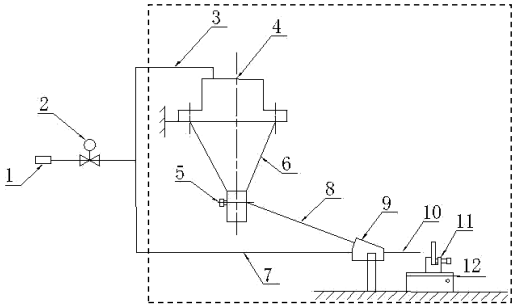


1-air compressor, 2-air pressure regulating valve, 3 and 7-air pipe, 4-vibrator, 5-sand regulating valve, 6-funnel, 8-sand tube, 9-gun, 10-jet, 11-sample holder, 12-angle adjuster

Fig.1 Schematic of self-designed AS600 sandblasting test machine

were $Al_2O_3$ angular particles with an average size of 80 μm. The SEM micrograph and EDS spectrum of the $Al_2O_3$ particles are shown in Fig.2.

## 2 Results and Discussion

### 2.1 Morphology of CrAlN coating

The surface and cross-section morphologies of the CrAlN coatings deposited by cathodic arc ion plating technology under various bias voltages are shown in Fig.3. All the coatings exhibit an analogous morphology with some macro-particles and pinholes on the surface. The macro-particles are mainly formed by the evaporated droplets, owing to the uneven movement of the arc spot on the surface of the target. The formation of the pinholes is mainly caused by the difference of the thermal expansion coefficients between the macro-particles and coatings[14]. The size and quantity of these macro-particles and pinholes are related to process parameters such as deposition pressure, substrate temperature, arc current, and bias voltage.

It can be found out that when the bias voltage is 0 V (Fig.3a) during the deposition, a lot of macro-particles form, leading to

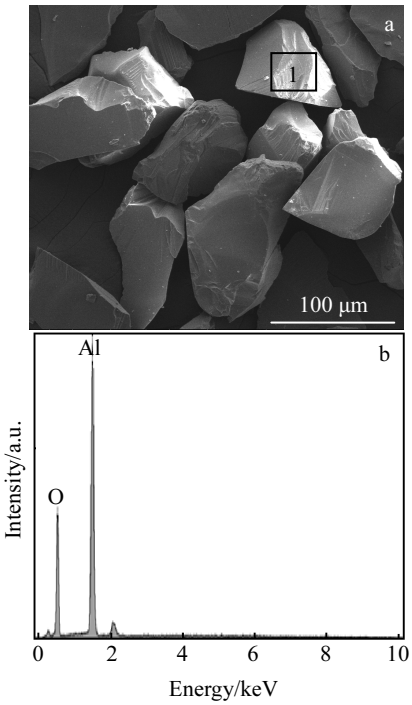


Fig.2 SEM image of surface morphology (a) and EDS spectrum of alumina ($Al_2O_3$) angular particles (b)

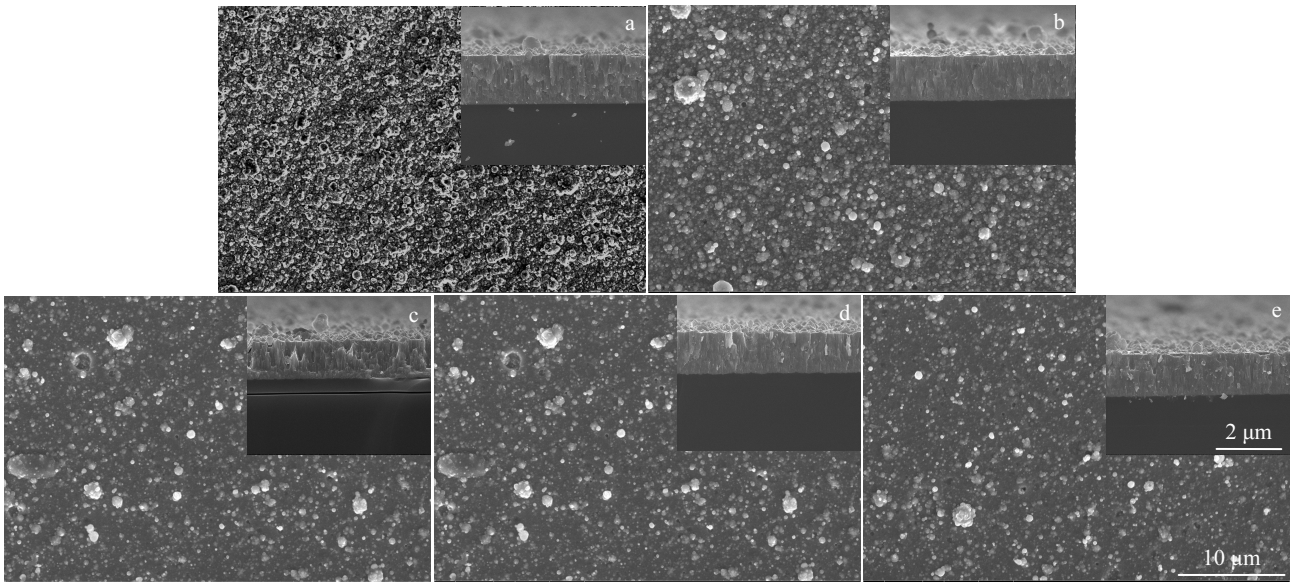


Fig.3 Surface and cross-section morphologies of CrAlN coatings under various bias voltages: (a) 0 V, (b) 50 V, (c) 100 V, (d) 150 V, and (e) 200 V

a rough surface. As the bias voltage increases, the number of macro-particles significantly decreases at 100 (Fig.3c), 150 (Fig.3d) and 200 V (Fig.3e). Meantime, the average size of the large particles is also reduced. It should be noted that with the increase of bias voltage, the purification effect of macro-particles on the surface of CrAlN coating is enhanced. At the same time, it can be seen from the cross-sectional morphology that the coatings are columnar microstructure, and the structure becomes increasingly finer and continuous at bias voltage of 150 V. The improvement of morphology should be attributed to higher bias voltage and ion energy. The higher bias voltage will generate more negative charges on the surface of the macro-particles, resulting in an increased repulsive force between particles and negative bias electric field of the substrate, thereby hindering the deposition of macro-particles. Meanwhile, the ion energy increases in the deposition process under the action of a larger negative bias. The incidence on the surface of the coating causes the macro-particles on the coating to be squeezed, thereby forming smaller particles.

### 2.2 Thickness and elemental composition of CrAlN coatings

The thickness, deposition rate, and Al, Cr content of CrAlN coatings is shown in Table 1, from which it can be seen that the thickness of the coatings decreases gradually at bias voltage of 0 V to −200 V, and the deposition rate is low. The increase of the bias voltage can enhance the energy of the deposited particles, thereby tamping the coating and increasing adhesion. In the deposition process, the coating is subjected to a certain sputtering cleaning effect, that is, a re-sputtering one. Therefore, the deposition rate of the coatings is reduced with increasing the bias voltage.

The alloy target Cr50Al50 was used in this work. Theoretically, the amount of deposited Cr and Al elements emitted by the arc should be the equal. However, as shown in Table 1, the Cr and Al contents in the coating are inconsistent. The ratio of Al to CrAl gradually increases at bias voltages from 50 V to 200 V, which also indicates that a part of the Cr and Al atoms deposited on the substrate are re-sputtered under the effect of the bias voltage. The difference of Cr and Al contents in coatings can be attributed to different sputtering yields of Cr and Al elements.

### 2.3 Crystallographic structure

Fig.4 shows XRD patterns of CrAlN coatings under various bias voltages. It can be seen that the crystal structures of CrAlN coatings are predominantly cubic crystal of CrN. The diffraction peaks of CrAlN coatings are mainly (111), (200), and (220) crystal planes, as shown in Fig.4. In addition, there is a superposition of the base peaks and some impurity peaks are not marked. As the substrate bias voltage increases, the diffraction peak of the crystal plane (200) in CrAlN coating broadens and the intensity gradually decreases. Notwithstanding, the intensity of the diffraction peak of the crystal plane (111) is enhanced. According to XRD patterns, combined with

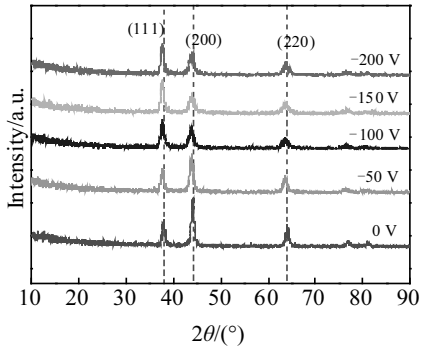


Fig.4 XRD patterns of CrAlN coatings under various bias voltages

the peak intensity and the texture coefficient of the crystal plane, it can be found that the preferred growth orientation of the CrAlN coating gradually changes from crystal plane (200) to crystal plane (111).

According to the report of Abadias et al [15], the energy of the entire coating surface is minimized by forming a new crystal island on its surface. In this study, the orientation of the (200) plane has the lowest surface energy, while (111) plane processes the lowest strain energy in the coating. Based on the energy minimization principle, the surface with the lowest surface energy or the lowest strain energy will grow preferentially [16]. Therefore, the coating will grow along the orientation of the (200) and (111) crystal plane. The results show that the growth orientations of CrAlN coatings are strongly related to the negative bias voltage. Increase in coating thickness and additional kinetic or thermal energy brought in the deposition process will introduce higher strain energy, resulting in the variation of coating orientation [17]. The relationship between ion kinetic energy and bias voltage is expressed as follows[18]:

$$U_{\mathrm{k}} \propto \frac{D_{\mathrm{w}} V_{\mathrm{b}}}{P_{1/2}} \tag{1}$$

where $U_{\mathrm{k}}$ is the ion kinetic energy, $D_{\mathrm{w}}$ is the target power density, $V_{\mathrm{b}}$ is negative bias voltage, and $P$ is the vacuum chamber gas pressure. As $V_{\mathrm{b}}$ increases, the ionic state acquires higher kinetic energy and transfers ions to the surface of the coating, while the ions diffuse rapidly. During this process, these attached atoms stick together, causing the rearrangement of the lattice atoms, as well as a considerable strain. In order to minimize the cumulative strain, the attached atoms will grow as much as possible along the less stressed plane. Thus, when a high bias voltage is applied, the energy of the ion stream increases and the ion bombardment substrate is enhanced. The coating produces a higher strain energy, which is converted into a preferential growth of the (111) crystal plane and has a minimum strain energy.

The Scherrer formula [19] was used to calculate the grain sizes of coatings at crystal plane of (111), (200) and (220),

from which the average grain size of coatings can be evaluated. The calculation results of the dimensions are 15, 13, 11, 9 and 10 nm. It can be found out that the finest grain size at 150 V corresponds to the columnar crystal grain refinement result in the cross-sectional morphology.

The obvious AlN diffraction peak cannot be found out in Fig.4. It is believed that when the value of ratio of Al:(Cr+Al) is about 0.70, the CrAlN coating may be converted from face-centered cubic CrN to AlN [20]. It can be seen from Table 1 that the ratio of Al:(Cr+Al) is much lower than 0.70, so the unstable and brittle AlN hardly forms. Once Al atoms enter the crystal lattice of CrN, it will increase the density and hardness of the coating. Compared with XRD pattern of the standard CrN, there is a left shift of $2\theta$ diffraction peaks when increasing the bias voltage from 0 V to –200 V. This is attributed to the increase in residual stresses, and the similar results were also found by Wang et al [21]. Furthermore, the enhanced ion bombardment results in re-sputtering effects on the coating surface to change the ratios of Al to Cr to a higher values owing to the differences in sputtering yields between Al and Cr, which also results in a slight peak shift to lower $2\theta$ diffraction angles.

### 2.4 Hardness and elastic modulus

The value of hardness ($H$) and elastic modulus ($E$) of CrAlN coatings is shown in Table 1. With the increase of bias voltage, the hardness of the coatings increases from 15.1 GPa at 0 V to 20.0 GPa at 150 V. The hardness increases non-linearly, but tends to stabilize. The hardness of the coating is affected by various factors, such as surface morphology, micro-structure, elemental composition, internal stress, thickness. These factors are often competitive in their influence on the hardness. It is reported[22] that when the value of ratio of Al:(Cr+Al) is less than 0.60, the CrAlN coating is a typical solid solution CrN with face-centered cubic structure, and its hardness increases with the increase of the ratio. According to the surface morphology and XRD results, the enhanced ion bombardment intensity under high bias voltage benefits the density and the residual compressive stress of the coating, and also reduces the number of macro-particles on the surface, leading to the increase of hardness.

Fig.5 shows the variation of elastic strain to failure resistance ($H/E$) and plastic deformation resistance ($H^3/E^2$) calculated by hardness ($H$) and elastic modulus ($E$). With the increase of the bias voltage, the values of $H/E$ and $H^3/E^2$ increase in the range from 0 V to 150 V. The obvious increment is obtained at 100 V, and the values keep stable after further increasing the bias voltage to 200 V. It has been reported[23] that $H/E$ and $H^3/E^2$ are positively correlated with coating toughness and play an important role in anti-crack initiation. The results show that the CrAlN coatings have of better toughness at –100~ –200 V.

### 2.5 Sand particle erosion

Fig.6 shows the erosion rates of TC11 titanium alloy and

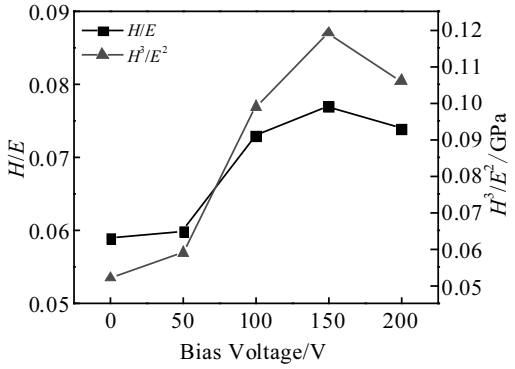


Fig.5 $H/E$ and $H^3/E^2$ as a function of the negative bias voltage for the CrAlN coatings

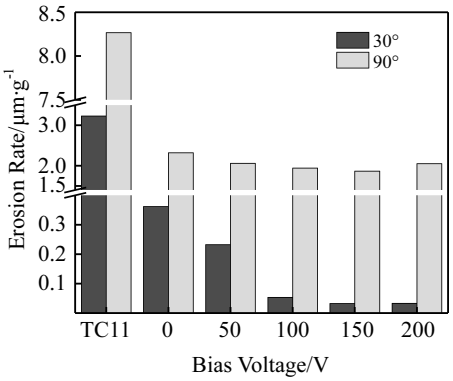


Fig.6 Solid particle erosion rates of TC11 and CrAlN coatings at various bias voltages

CrAlN coatings at 30° and 90° impact angles. The erosion rates are calculated based on how depth per gram of sand can be washed away in the erosion test. As can be seen from Fig.6, the TC11 titanium alloy keeps the erosion rate of 3.227 μm/g at 30° and 8.267 μm/g at 90°. The erosion resistance performance of the alloy with CrAlN coating is significantly higher than that of the uncoated specimen. The fastest erosion rate of the coated specimen appears at the bias voltage of 0 V, which is 0.362 μm/g at 30° and 2.322 μm/g at 90°. Even so, these erosion rates are only 1/9 and 1/3 of those of the uncoated sample at 30° and 90°, respectively. For the CrAlN coating specimens, the erosion resistance is improved at 30° and 90° angles with the increase of the bias voltage. The erosion resistance is remarkably strengthened when the bias voltage increases to 100 V, and it remains at 100~200 V. At 150 V, the minimum erosion rate is reached at both angles, 0.032 μm/g at 30° and 1.869 μm/g at 90°. It shows that the CrAlN coating has great erosion resistance when the bias voltage is high.

Fig.7 presents the morphology of CrAlN coating at the bias voltage of 150 V after a 90° sand scouring experiment. Fig.7a is a macro-view upon the erosion scar area, which is divided into four parts from the outside to the inside: unwashed area (intact

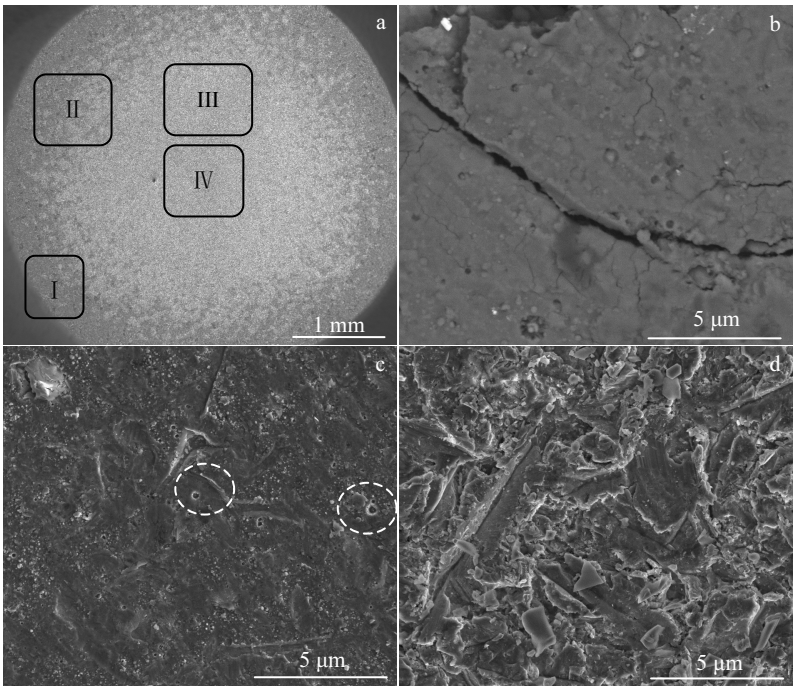


Fig.7 Morphologies of CrAlN coating at the bias voltage of 150 V after 90° sand scouring experiment: (a) macro-view of the erosion scar area, (b) area II, (c) area III, and (d) area IV

coating, I), edge washed area (elastic loading deformation, II), severe washed area (partial peeling of coating, III), and scoured center area (bare substrate, IV). Therefore, in the process of erosion, it is easy to understand that the coatings undergo the following four stages: (1) intact coating; (2) elastic loading deformation; (3) part of the coating begins to peel off; (4) the coating is completely peeled off and exposed to the substrate, corresponding to several aspects above.

Areas II, III, and IV are observed to further investigate the erosion process of the CrAlN coatings. Fig.7b is an enlarged version of area II in Fig.7a. When the coating is impacted in the vertical direction of the erosion particles, stress concentration and cracks may occur, and the coating is deformed as the crack propagates. As the erosion continues, some coatings in Fig.7c begin to peel off, while the pits (as marked in Fig.7c) left after the macro-particles falls off can be observed. Under the repeated impact of the erosion particles, the cracks continue to expand and connect with each other, eventually leading to the coating to peel off. Fig.7d shows the erosion morphology which seems like the typical titanium alloy, demonstrating that the coating is completely peeled off. It can be seen that the surface is extremely uneven. The erosion particles vertically impact the substrate, leaving a lot of pits being formed into steps by the deformed lips that are squeezed out. The exposed titanium alloy substrate undergoes the continuous vertical forging and produces cracks after repeated deformation and hardening, and final cracks and peels off as the crack propagates.

## 3 Discussion

It is generally considered that the effect of particles on brittle materials is caused by elastic/plastic fracture. In this erosion test, the solid particles are accelerated toward the surface of the coating. During the impact, the kinetic energy of the solid particles is absorbed by the coating and converted into the plastic deformation of the coating. Wherein, the surface transverse crack propagates outward from the bottom of the contact region on the plane basically parallel to the surface, and the intermediate crack propagates from the contact area perpendicular to the surface. The peeling of the final coating is caused by the interaction of transverse and radial cracks. It is generally considered that erosion of brittle materials have two material removal models: one is to remove tough pear cutting material; the other is the process of crack initiation, expansion, and removal. Both mechanisms are possible, depending on the specific stress state in the case of hard coatings currently under consideration. In this work, the CrAlN coating is mainly removed by crack initiation induction. The relationship between crack initiation, expansion and coating hardness, elastic modulus and toughness is inseparable. $H/E$ parameters determine the tribology properties of the material. In the meantime, $H^3/E^2$ ratio is the parameter that controls the material's resistance to plastic deformation [24]. The results show that the CrAlN coatings with a high $H/E$ and $H^3/E^2$ ratio exhibit

lower erosion rates.

In this study, the CrAlN coatings have different hardness, surface morphologies, composition, grain size and internal stresses due to various bias voltages during deposition. The hardness of the coating ensures the wear resistance. The small grain size plays an inevitably significant role in fine grain strengthening. The increase in compression stress allows the coating to store more impact energy without plastic deformation. Based on the characteristics of arc ion plating, more or less micron-sized droplets are present in the coating. These droplets are deposited on the substrate by the fusion spraying of the CrAl target, and the hardness is much lower than that of the CrAlN coating. The effect of the CrAl droplets embedded in the coating on the overall erosion resistance of the coating was analyzed. It is shown that ductile materials have the ability to passivate the crack tip and then to redistribute the strain through the plastic mechanism. However, Hsai et al[25] believe that ductile coatings with a thickness less than 1 μm are not allowed to emit effective dislocations from the near crack tip. Therefore, the droplets of the ductile phase have no effect on the crack propagation when the diameter is less than 1 μm. Another study [26] shows that in multilayer coatings with ductile phases, cracks can be redirected along the interface as the crack approaches the interface, and deflected at the interface, or stopped if the strain energy release rate changes significantly. However, it can also lead to premature stratification. In this work, this process is manifested as the droplet shedding, leaving behind surface defects that lead to a sudden increase in the erosion rate. As shown in Fig.6, the CrAlN coating (0 V) with a large number of surface droplets shows a higher erosion rate than the CrAlN coating (150 V) with a small number of droplets. Therefore, although large droplets of the ductile phase may play a role in deflecting cracks and absorbing stress, they generate larger defects and accelerate the erosion after shedding. Therefore, taking the surface morphology, composition, hardness, elastic modulus, grain size and residual stress of the coating into account, it is extremely important to select appropriate electrical parameters to prepare CrAlN coating with good erosion resistance.

## 4 Conclusions

1) When the bias voltage changes from 0 V to 200 V, the preferred growth orientation of the CrA1N coating gradually changes from (200) to (111) crystal plane. The hardness increases from 15.1 GPa to about 20 GPa, adhesion increases to 42.6 N, the surface gradually flattens, and the number of macro-particles and pinholes decreases.

2) With the increase of bias voltage, the erosion resistance of CrAlN coating gradually improves. At 30° and 90° erosion angles, the maximum erosion rate of the CrAlN coated samples is only 1/9 and 1/3 of that of the titanium alloy. The CrAlN coating formed at a bias voltage of 150 V has the minimum erosion rate of 0.032 μm/g at 30° and 1.869 μm/g at 90°.

3) The erosion and fracture mechanism of CrAlN coating as brittle material is discussed. On the one hand, the impact of the coating causes stress concentration and cracks; on the other hand, the impact process causes macro-particles on the surface to fall off, leaving deep pits to promote the crack propagation. Good surface quality, small number of droplets, fine grain size and high $H/E$ and $H^3/E^2$ ratio are key factors in defending the solid particle erosion, indicating that the increase of the erosion resistance of CrAlN coatings can be achieved by appropriately controlling negative bias voltage.

## References


1 Hamed A, Tabakoff W C, Wenglarz R V. *Journal of Propulsion & Power*[J], 2012, 22(2): 350

2 Bousser E, Martinu L, Klemberg-Sapieha J E. *Surface & Coatings Technology*[J], 2014, 257: 165

3 Lin Songsheng, Zhou Kesong, Dai Mingjiang *et al*. *Vacuum*[J], 2015, 122: 179

4 Deng Jianxin, Wu Fengfang, Lian Yunsong *et al*. *International Journal of Refractory Metals & Hard Materials*[J], 2012, 35: 10

5 Wang Qianzhi, Zhou Fei, Yan Jiwang. *Surface & Coatings Technology*[J], 2016, 285: 203

6 Reedy M W, Eden T J, Potter J K *et al. Surface & Coatings Technology*[J], 2011, 206(2-3): 464

7 Bose K, Wood R J K, Wheeler D W. *Wear*[J], 2005, 259(1-6): 135

8 Wheeler D W, Wood R J K. *Wear*[J], 2001, 250(1-12): 795

9 Wang Quanhong, Dai Mingjiang, Liu Libin *et al*. *China Surface Engineering*[J], 2012, 25(1): 22 (in Chinese)

10 Borawski B, Singh J, Todd J A *et al*. *Wear*[J], 2011, 271(11-12): 2782

11 Song G H, Luo Z, Feng L I *et al*. *Transactions of Nonferrous Metals Society of China*[J], 2015, 25(3): 811

12 Polcar T, Cavaleiro A. *Surface & Coatings Technology*[J], 2011, 206(6): 1244

13 ASTM. *Standard Test Method for Conducting Erosion Tests by Solid Particle Impingement Using Gas Jets,* G76-13[S]. ASTM, 2013

14 Kumagai M, Yukimura K, Kuze E *et al*. *Surface & Coatings Technology*[J], 2003, 169(22): 401

15 Abadias G. *Surface & Coatings Technology*[J], 2008, 202(11): 2223

16 Pelleg J, Zevin L Z, Lungo S *et al*. *Thin Solid Films*[J], 1991, 197(1-2): 117

17 Detor A J, Hodge A M, Chason E *et al*. *Acta Materialia*[J], 2009, 57(7): 2055

18 Zhang M, Li M K, Kim K H *et al*. *Applied Surface Science*[J], 2009, 255(22): 9200

19 Hirsch P B. *Physics Bulletin*[J], 1957, 8(7): 237

20 Reiter A E. *Surface & Coatings Technology*[J], 2005, 200(7): 2114

21 Wang Y X, Zhang S, Lee J W *et al*. *Surface & Coatings*

*Technology*[J], 2012, 206(24): 5103
22 Barshilia H C, Selvakumar N, Deepthi B *et al*. *Surface & Coatings Technology*[J], 2006, 201(6): 2193
23 Ou Y X, Lin J, Che H L *et al. Surface & Coatings Technology*[J], 2015, 276: 152
24 Shtansky D V, Kiryukhantsev-Korneev P V, Bashkova I A *et al. International Journal of Refractory Metals & Hard Materials*[J], 2010, 28(1): 32
25 Hsia K J, Suo Z, Yang W. *Journal of the Mechanics & Physics of Solids*[J], 1994, 42(6): 877
26 Dück A, Gamer N, Gesatzke W *et al. Surface & Coatings Technology*[J], 2001, 142(1): 579

# 偏压对电弧离子镀 CrAlN 涂层微观结构及耐侵蚀性能的影响

王 迪[1,2]，林松盛[2]，刘灵云[2]，薛玉娜[1]，杨洪志[2]，蒋百灵[1]，周克崧[1,2]
(1. 西安理工大学，陕西 西安 710048)
(2. 广东省新材料研究所 现代材料表面工程技术国家工程实验室 广东省现代表面工程技术重点实验室，广东 广州 510651)

**摘 要**：通过在 TC11 钛合金上利用电弧离子镀技术制备了铬铝氮（CrAlN）涂层。采用 X 射线衍射（XRD），扫描电子显微镜（SEM），能量色散 X 射线光谱（EDS），纳米压痕仪等对 CrAlN 涂层微观结构和力学性能（如硬度和弹性模量）进行了分析。为了研究偏压对 CrAlN 涂层固体颗粒耐侵蚀性的影响，还进行了一系列固体颗粒侵蚀实验。结果发现，随着偏压从 0 V 增加至 200 V，CrA1N 涂层的择优生长取向逐渐从（200）转变为（111）晶面。硬度从 15.1 GPa 增加至接近 20 GPa。同时，表面逐渐平整，大颗粒和针孔的数量减少，对 CrAlN 涂层的耐侵蚀性能均有一定影响。偏压 150 V 时，CrAlN 涂层获得最小侵蚀速率，其在 30° 时为 0.032 μm/g，90° 时为 1.869 μm/g。这些结果表明，选择适当的偏压，CrAlN 涂层能够获得更优异的固体颗粒耐侵蚀性。

**关键词**：CrAlN 涂层；负偏压；微观结构；固体颗粒侵蚀

---

作者简介：王 迪，男，1991 年生，博士，西安理工大学材料科学与工程学院，陕西 西安 710048，电话：029-61086553，E-mail: 343585114@qq.com